# Kinetics of two-step catalytic sequence on nanoclusters with limited cluster occupancy

Murzin, Dmitry Yu

*Published in:*
Chemical Engineering Journal

*DOI:*
10.1016/j.cej.2022.138178

Published: 15/12/2022

*Document Version*
Final published version

Chemical Engineering Journal 450 (2022) 138178

Contents lists available at ScienceDirect

Chemical Engineering Journal

journal homepage: www.elsevier.com/locate/cej

# Kinetics of two-step catalytic sequence on nanoclusters with limited cluster occupancy

Dmitry Yu. Murzin

*Åbo Akademi University, Henriksgatan 2, 20500 Åbo/Turku, Finland*

A B S T R A C T

Two-step catalytic sequence was considered for cooperative kinetics of heterogeneous catalytic reactions on nanoclusters with a limited number of adsorbed species due to size restrictions allowing for derivation of the corresponding rate expressions. Dependence of the kinetic parameters on the number of adsorbed species was considered for different models of biographical (intrinsic) and induced non uniform surfaces. Explicit expressions were derived for the rates on evenly nonuniform surfaces exhibiting a linear decrease in the Gibbs energy with site occupancy. An expression for the apparent activation energy was obtained for the two step sequence with both irreversible steps. Simulations were performed for several expressions for the forward reaction rate in a two-step sequence with different number of maximal adsorbed species. The analysis illustrated that the reaction rates in the forward direction pass through maxima even without any competition of both reactants. Strong nonuniformity or lateral interactions make the rate maxima less prominent. Larger clusters, which can accommodate more adsorbed intermediates per cluster, exhibit rather wide maxima in the rates expanding over a broad range of concentrations.

The experimental data on resazurin reduction with hydroxylamine over gold clusters bearing 15 to 25 gold atoms were used to illustrate applicability of the developed theoretical approach showing a dramatic switch in kinetic regularities between Au15 and Au18 clusters, which could be attributed to changes in the number of adsorbed species per cluster.

## 1. Introduction

Recent development in nanocatalysis combined with significant advancements in preparation and characterization methods of nanoclusters inspired a renewed interest in theoretical kinetic analysis of the respective reactions [1–6]. It is apparently clear that the conventional approaches based on the pioneering work of Langmuir with metal films [7] and subsequent contributions of Horiuti [8] and Temkin [9], who studied predominantly bulk metals/oxides as catalysts, cannot be directly applied to nanocatalysis. The main conceptual objection is related to utilization of the concept of surface coverage and fast surface diffusion, which is questionable as only few reacting molecules can be adsorbed on a nanocluster. As an illustration, let us consider a semispherical metal cluster of a dimeter of 1.5 nm. The surface area of such a cluster being ca. 3.5 $nm^2$ implies that if the maximum cross section of a molecule is in the range ca. 0.3–0.5 $nm^2$/molecule [10], which are typical values for hydrocarbons with just 4–7 carbon atoms, a limited number of molecules (6–10) can be adsorbed on a single cluster. For large organic molecules, like betulin [11], there could be just 2–3 adsorbed molecules per cluster.

In the ultimate case of single-atom catalysts with 100 % surface utilization [12–14] the concept of surface coverage on a particular cluster does not hold as a particular catalytic site is either empty or is occupied taking part in a catalytic cycle. To address this apparent inconsistency with classical catalytic kinetics, stochastic kinetic models for the Michaelis-Menten kinetics with enzymes [15,16] or conceptually similar Eley-Rideal kinetics [17] have been advanced for single site catalysts. Surprisingly even for single nanocatalysts different catalytic sites might influence each other [18], because of cooperative behavior. The stochastic kinetics was also used for linear sequences on a single nanocatalyst with multiple active sites operating independent on each other [19]. When the stochastic effects are averaged, the nanocatalyst with multiple active sites behaves as an effective catalyst with a single site.

A different approach was developed in [20,21], explicitly considering adsorption equilibria on metal clusters with a finite number of adsorbed molecules per a single metal cluster. Considerations of a two-step sequence with the first step of adsorption being in quasi- equilibria and a second rate determining step resulted in a rate expression with polynomial terms in the nominator and the denominator [21]

$$r = \frac{a_1 C_A + a_2 C_A^2 + \ldots + a_n C_A^n}{1 + b_1 C_A + b_2 C_A^2 + \ldots + b_n C_A^n} = \frac{\sum_1^n a_n C_A^n}{1 + \sum_1^n b_n C_A^n} \quad (1)$$

In eq. (1) $n$ is the number of adsorbed molecules per cluster, $a_i$ stands for terms containing kinetic and adsorption constants, while $b_i$ is related to adsorption terms. Eq. (1) was derived [21] assuming that all kinetic

*E-mail address:* dmurzin@abo.fi.

https://doi.org/10.1016/j.cej.2022.138178
Received 3 June 2022; Received in revised form 10 July 2022; Accepted 16 July 2022
Available online 21 July 2022

and adsorption constants depend on the spatial arrangements of reacting molecules. On the contrary, for the two-step sequence with one most abundant surface intermediate, mechanistically close to the Eley-Rideal mechanism,

$$\begin{array}{l} 1.\ * + \mathrm{A} \leftrightarrow \mathrm{I}^* + \mathrm{C} \\ 2.\ \dfrac{\mathrm{I}^* + \mathrm{B} \leftrightarrow * + \mathrm{D}}{\mathrm{A} + \mathrm{B} \leftrightarrow \mathrm{C} + \mathrm{D}} \end{array} \tag{2}$$

the same rate constants on a bare surface and occupied clusters were considered independent on the number of adsorbed species [21]. In eq. (2) often used for description of experimental data in heterogeneous catalysis [22,23] *A, B, C* and *D* are reactants, and *I* is an adsorbed intermediate.

The general form for the two-step sequence with *n* adsorbed reaction intermediates is [21]

$$r = \frac{\omega_{+1}(1 + U + U^2 + ... + U^{n-1}) - \omega_{-1}(U + U^2 + ... + U^n)f_{total}}{1 + U + U^2 + ... + U^n} \tag{3}$$

where

$$U = \frac{k_{+1}C_A + k_{-2}C_D}{k_{+2}C_B + k_{-1}C_C} = \frac{\omega_{+1} + \omega_{-2}}{\omega_{+2} + \omega_{-1}} \tag{4}$$

$f$ is the total number of metal clusters and $\omega_{+1}$ etc. are frequencies of steps [22], e.g.$\omega_{+1} = k_{+1}C_A; \omega_{-1} = k_{-1}C_C$, etc. It can be easily demonstrated based on the steady state approximation for eq. (2) $k_{+1}C_A\theta_0 - k_{-1}C_C\theta_I = k_{+2}C_B\theta_I - k_{-2}C_D\theta_0$ where $\theta_I$ and $\theta_0$ are respectively the coverage of the intermediate *I* and the fraction of empty sites, that the parameter U corresponds to their ratio (i.e. $U = \theta_I/\theta_0$).

An extension of this theoretical development was recently done for a case when the surface of a nanocluster can accommodate only two adsorbed reaction intermediates [24]. A more general approach, however, requires analysis of the cases when many more molecules can adsorb on a cluster and that kinetic parameters are dependent on the occupancy of a cluster.

## 2. Two-step sequence

The treatment in [21,24] assumes that due to cooperative behavior in catalytic reactions over nanoclusters, the reaction mechanism (i.e. eq. (2)) should be modified to include as many reaction routes as the number of adsorbed molecules /intermediates that a cluster can accommodate. In [24] two adsorbed species per cluster were considered resulting in a following rate equation:

$$\begin{aligned} r = r = \frac{(\omega^I_{+1}\omega^I_{+2} - \omega^I_{-1}\omega^I_{-2} + (\omega^{II}_{+1}\omega^{II}_{+2} - \omega^{II}_{-1}\omega^{II}_{-2})\dfrac{\omega^I_{+1} + \omega^I_{-2}}{\omega^{II}_{+2} + \omega^{II}_{-1}})f_{total}}{\omega^I_{+1} + \omega^I_{+2} + \omega^I_{-1} + \omega^I_{-2} + (\omega^I_{+1} + \omega^I_{-2})\dfrac{\omega^{II}_{+1} + \omega^{II}_{-2}}{\omega^{II}_{+2} + \omega^{II}_{-1}}} = \\ = \frac{(\omega^I_{+1} + \omega^{II}_{+1}U_1 - \omega^I_{-1}U_1 - \omega^{II}_{-1}U_1U_2)f_{total}}{1 + U_1 + U_1U_2} \end{aligned} \tag{5}$$

with

$$U_1 = \frac{\omega^I_{+1} + \omega^I_{-2}}{\omega^I_{+2} + \omega^I_{-1}}; U_2 = \frac{\omega^{II}_{+1} + \omega^{II}_{-2}}{\omega^{II}_{+2} + \omega^{II}_{-1}} \tag{6}$$

A more illustrative example is provided below with maximum four adsorbed intermediates due to spatial availability on a nanocluster (Fig. 1).

The mechanism for such case can be rewritten in the following way:

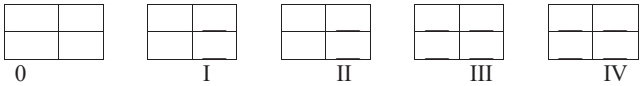


**Fig. 1.** Clusters with up to four adsorbed species for the mechanism in eq. (5).

| | N(I) | N(II) | N(III) | N(IV) |
|---|---|---|---|---|
| I.1 $* + \mathrm{A} \leftrightarrow \mathrm{I}^* + \mathrm{C}$ | 1 | 0 | 0 | 0 |
| I.2 $\mathrm{I}^* + \mathrm{B} \leftrightarrow * + \mathrm{D}$ | 1 | 0 | 0 | 0 |
| II.1 $\mathrm{I}^* + \mathrm{A} \leftrightarrow \mathrm{II}^* + \mathrm{C}$ | 0 | 1 | 0 | 0 |
| II.2 $\mathrm{II}^* + \mathrm{B} \leftrightarrow \mathrm{I}^* + \mathrm{D}$ | 0 | 1 | 0 | 0 |
| III.1 $\mathrm{II}^* + \mathrm{A} \leftrightarrow \mathrm{III}^* + \mathrm{C}$ | 0 | 0 | 1 | 0 |
| III.2 $\mathrm{III}^* + \mathrm{B} \leftrightarrow \mathrm{II}^* + \mathrm{D}$ | 0 | 0 | 1 | 0 |
| IV.1 $\mathrm{III}^* + \mathrm{A} \leftrightarrow \mathrm{IV}^* + \mathrm{C}$ | 0 | 0 | 0 | 1 |
| IV.2 $\mathrm{IV}^* + \mathrm{B} \leftrightarrow \mathrm{III}^* + \mathrm{D}$ | 0 | 0 | 0 | 1 |

(7)

where the numbers (0 or 1) correspond to the stoichiometric numbers (i.e. Horiuti numbers) of a particular step in the corresponding reaction route [25,26]. As expected four reaction routes in eq. (5) give the same chemical equation. The concentration of clusters having different number of adsorbed intermediates (Fig. 1) $f_0, f_1 - f_4$ can be computed based on the steady state approximations for the reactions routes $\mathrm{N^{(I)}}$ - $\mathrm{N^{(IV)}}$ respectively:

$$\begin{aligned} r^I_{+1} - r^I_{-1} = r^I_{+2} - r^I_{-2}; r^{II}_{+1} - r^{II}_{-1} = r^{II}_{+2} - r^{II}_{-2}; r^{III}_{+1} - r^{III}_{-1} = r^{III}_{+2} - r^{III}_{-2}; r^{IV}_{+1} - r^{IV}_{-1} \\ = r^{IV}_{+2} - r^{IV}_{-2} \end{aligned} \tag{8}$$

Giving subsequently:

$$k^I_{+1}C_Af_0 - k^I_{-1}C_Cf_1 = k^I_{+2}C_Bf_1 - k^I_{-2}C_Df_0 \tag{9}$$

$$k^{II}_{+1}C_Af_1 - k^{II}_{-1}C_Cf_2 = k^{II}_{+2}C_Bf_2 - k^{II}_{-2}C_Df_1 \tag{10}$$

$$k^{III}_{+1}C_Af_2 - k^{III}_{-1}C_Cf_3 = k^{III}_{+2}C_Bf_3 - k^{III}_{-2}C_Df_2 \tag{11}$$

$$k^{IV}_{+1}C_Af_3 - k^{IV}_{-1}C_Cf_4 = k^{IV}_{+2}C_Bf_4 - k^{IV}_{-2}C_Df_3 \tag{12}$$

The ratio between the concentration of clusters can easily derived from eq. (9–12), namely

$$f_1 = U_1f_0; f_2 = U_1U_2f_0; f_3 = U_1U_2U_3f_0; f_4 = U_1U_2U_3U_4f_0 \tag{13}$$

Where $U_1$ and $U_2$ are expressed by eq. (6) and

$$U_3 = \frac{\omega^{III}_{+1} + \omega^{III}_{-2}}{\omega^{III}_{+2} + \omega^{III}_{-1}}; U_4 = \frac{\omega^{IV}_{+1} + \omega^{IV}_{-2}}{\omega^{IV}_{+2} + \omega^{IV}_{-1}} \tag{14}$$

The mass balance of clusters having different amounts of adsorbed species is

$$f_0 + f_1 + f_2 + f_3 + f_4 = f_{total} \tag{15}$$

Which gives an expression for the bare clusters concentration

$$f_0 = \frac{f_{total}}{1 + U_1 + U_1U_2 + U_1U_2U_3 + U_1U_2U_3U_4} \tag{16}$$

The overall reaction rate along four routes is the sum of the rates of these routes [9]

$$r = r^{(I)} + r^{(II)} + r^{(III)} + r^{(IV)} = r^I_{+1} - r^I_{-1} + r^{II}_{+1} - r^{II}_{-1} + r^{III}_{+1} - r^{III}_{-1} + r^{IV}_{+1} - r^{IV}_{-1} \tag{17}$$

which can be rewritten as

$$r = r^I_{+1} + r^{II}_{+1} + r^{III}_{+1} + r^{IV}_{+1} - r^I_{-1} - r^{II}_{-1} - r^{III}_{-1} - r^{IV}_{-1} \tag{18}$$

In eq. (18) $r_+$ and $r_-$ are the overall rates in the forward and reverse directions respectively. In eq. (17) the rates of the first steps along different routes are selected. It is apparently clear that the same result follows if the second step would be considered, because the reaction is under steady state conditions.

The rate in the forward direction is the sum of the rates in the forward direction for all routes.

$$r_+ = k^I_{+1}C_A f_o + k^{II}_{+1}C_A f_1 + k^{III}_{+1}C_A f_2 + k^{IV}_{+1}C_A f_3 = \\ = k^I_{+1}C_A f_o + k^{II}_{+1}C_A U_1 f_0 + k^{III}_{+1}C_A U_1 U_2 f_0 + k^{IV}_{+1}C_A U_1 U_2 U_3 f_0 = \\ = \frac{(k^I_{+1} + k^{II}_{+1}U_1 + k^{III}_{+1}U_1U_2 + k^{IV}_{+1}U_1U_2U_3)C_A f_{total}}{1 + U_1 + U_1U_2 + U_1U_2U_3 + U_1U_2U_3U_4} \quad (19)$$

Or

$$r_+ = \frac{(\omega^I_{+1} + \omega^{II}_{+1}U_1 + \omega^{III}_{+1}U_1U_2 + \omega^{IV}_{+1}U_1U_2U_3)f_{total}}{1 + U_1 + U_1U_2 + U_1U_2U_3 + U_1U_2U_3U_4} \quad (20)$$

The rate in the reverse direction is then:

$$r_- = \frac{(\omega^I_{-1}U_1 + \omega^{II}_{-1}U_1U_2 + \omega^{III}_{-1}U_1U_2U_3 + \omega^{IV}_{-1}U_1U_2U_3U_4)f_{total}}{1 + U_1 + U_1U_2 + U_1U_2U_3 + U_1U_2U_3U_4} \quad (21)$$

The overall rate for the mechanism in eq. (7) is

$$r = \frac{(\omega^I_{+1} + \omega^{II}_{+1}U_1 + \omega^{III}_{+1}U_1U_2 + \omega^{IV}_{+1}U_1U_2U_3 - \omega^I_{-1}U_1 - \omega^{II}_{-1}U_1U_2 - \omega^{III}_{-1}U_1U_2U_3 - \omega^{IV}_{-1}U_1U_2U_3U_4)f_{total}}{1 + U_1 + U_1U_2 + U_1U_2U_3 + U_1U_2U_3U_4} \quad (22)$$

Or

$$r = \frac{(\omega^I_{+1} + \omega^{II}_{+1}U_1 + \omega^{III}_{+1}U_1U_2 + \omega^{IV}_{+1}U_1U_2U_3)(1 - \frac{\omega^I_{-1}U_1 + \omega^{II}_{-1}U_1U_2 + \omega^{III}_{-1}U_1U_2U_3 + \omega^{IV}_{-1}U_1U_2U_3U_4}{\omega^I_{+1} + \omega^{II}_{+1}U_1 + \omega^{III}_{+1}U_1U_2 + \omega^{IV}_{+1}U_1U_2U_3})f_{total}}{1 + U_1 + U_1U_2 + U_1U_2U_3 + U_1U_2U_3U_4} \quad (23)$$

which can be presented as

$$r = r_+(1 - \frac{r_-}{r_+}) \quad (24)$$

For the reaction mechanism in eq. (7) the ratio between the rates in the reverse and forward directions is equal to the equilibrium constant of the chemical equation, which is the same for all routes. Subsequently this ratio is equivalent to the expression, which follows from the treatment of Horiuti [25] for a reversible reaction without a rate-limiting step and the stoichiometric number of all steps equal to unity:

$$\frac{r_-}{r_+} = \frac{1}{K}\frac{C_C C_D}{C_A C_B} \quad (25)$$

Apparently, a general equation for the $n$ species adsorbed on the catalyst surface can be easily written in a similar form as eq. (21)

$$r_+ = \frac{(\omega^I_{+1} + \omega^{II}_{+1}U_1 + \omega^{III}_{+1}U_1U_2 + .. + \omega^n_{+1}U_1U_2..U_{n-1})f_{total}}{1 + U_1 + U_1U_2 + U_1U_2U_3 + ... + U_1U_2U_3...U_n} \quad (26)$$

The rate in the reverse direction in a general form can be presented in a following way

$$r_- = \frac{(\omega^I_{-1}U_1 + \omega^{II}_{-1}U_1U_2 + \omega^{III}_{-1}U_1U_2U_3 + .. + \omega^n_{-1}U_1U_2..U_n)f_{total}}{1 + U_1 + U_1U_2 + U_1U_2U_3 + ... + U_1U_2U_3...U_n} \quad (27)$$

Applicability of eq. (25) can be easily demonstrated for the case of one adsorbed species per cluster being expanded in [24] to the case of clusters with up to two adsorbed species on a two-site ensemble (e. 5). A more tedious derivation resulting in the equation of Horiuti can be done for the case of several routes considering that the overall equilibrium constant is independent on the number of adsorbed species on a cluster.

## 3. Cluster occupation dependence

As can be seen from eq. (26) and (27) there is a substantial number of parameters, which describe the reaction rates, making both expressions very difficult to tackle especially for a reasonably large number of adsorbed species per cluster $n$ when the adsorption or kinetic parameters vary depending on $n$. Such variations are expected, when there is a distribution of sites with different reactivity or lateral interactions are present.

Dependence of the rate parameters on the size and shape of metal clusters has been considered previously theoretically [27–30] and for specific reactions [31–34].

In general, structure sensitive reactions are analyzed independent on kinetics [29,30] or by incorporating the cluster size dependence in the expressions for rate constants [27,30]. In the former case no dependence of the rate constants on the cluster size or shape is assumed, and the adsorption/desorption or reaction rates are calculated considering the fraction of terraces, edges and corners of different reactivity depending on the cluster size. This approach obviously does not consider explicitly the reaction mechanisms. An alternative method is to apply the thermodynamic approach [27] implying that the equilibrium constants of adsorption can be computed through size/shape dependent Gibbs adsorption energy. Subsequently the linear free energy (or Brønsted-Evans-Polanyi) relationship between the reaction constants $k$ and equilibrium constants $K$ is applied in the form $k = g\ K^{\alpha}$ where g and α (Polanyi parameter, $0 < \alpha < 1$) are constants.

The thermodynamic approach considers how the chemical potential of a nanocluster changes as a function of the cluster size [35]. In general the chemical potential is the amount by which the Gibbs energy of the system changes if an additional particle was introduced, with the pressure and temperature fixed. A basic thermodynamic equation for a macroscopic system connecting incremental changes in energy, heat and work is.

$$dG = Vdp - SdT + \sum_{i=1}^{k}\mu_i dN_i + \gamma' dA \quad (28)$$

where $\mu_i$ is the chemical potential of the $i$th chemical compound, $N_i$ is the number of particles (or number of moles) composing the $i$th chemical component, A is the surface and γ' is the surface energy excess. The latter defines the relationship between the amount of work performed in enlarging a surface and the surface area created.

In the context of the current work, the interest is on the impact of the quantity of adsorbed species per cluster on the chemical potential. In [36] two contributions to the chemical potential were considered, the intrinsic one related to the cluster size and the induced part because of the excess surface energy changes upon adsorption.

Corresponding differences in the values of kinetic parameters with an increase of the number of adsorbed species are thus ascribed also to either distribution of sites with different binding strength or lateral interactions between adsorbed species. In the first case obviously the sites exhibiting stronger affinity to the adsorbate will be occupied first followed by filling the sites which adsorb less strongly. The lateral

interactions imply that repulsive or attractive interactions upon adsorption are manifested also changing the adsorption energy depending on the site occupancy.

Subsequently differences in say $\omega_{+1}^{I}$ , $\omega_{+1}^{II}$ and $\omega_{+1}^{n}$ originate from biographical (intrinsic) and induced nonunuformity [9]. In the literature different models were considered to account for both types of nonuniformity. A linear decrease of the adsorption heat as a function of coverage corresponds to the so-called evenly nonuniform surfaces and the logarithmic adsorption isotherm [9], while deviations from linearity result in the Freundlich isotherm [37]. A conceptually different view on real adsorbed layer implying lateral interactions in the simplest form assumes also a linear decrease of adsorption energy ε on coverage θ within the concept of the surface electronic gas [9]

$$\varepsilon = \varepsilon^0 - \frac{\eta^2 h^2 L}{4\pi m^*}\theta \tag{29}$$

where η is the effective charge acquired by an adsorbed particle, $h$ is the Plank constant, L is the number of adsorption sites on the unit surface, m* effective electron mass. Eq. (29) leading to the Fowler- Guggenheim adsorption isotherm [1,38] could be presented in a more general form [39] for adsorption of species $A$

$$\varepsilon = \varepsilon^0 - w_{AA} n_1 \tag{30}$$

where $w_{AA}$ is the energy of $A$-$A$ lateral interactions between nearest neighbors and $n_1$ is the number of nearest-neighbor interactions. A more complex dependence implies also that lateral interactions between next-nearest-neighbors should be considered as well

$$\varepsilon = \varepsilon^0 - w_{AA} n_1 - w_{AA'} n_2 \tag{31}$$

where $n_1$ is the number of next-nearest-neighbor sites.

Both models (i.e. intrinsic and induced nonuniformity) imply a decrease of adsorption heat as a function of the site occupancy. In the context of the current work considering adsorption on nanoclusters with a limited number of adsorbed species per cluster, adsorption energy should be viewed as a function of the average number of adsorbed species per cluster across all clusters.

When the interval between the maximum and minimum values of the Gibbs adsorption energy can be defined in the following way [9]

$$\psi = \frac{\Delta G_{ads,\min} - \Delta G_{ads,\max}}{RT} \tag{32}$$

and a relative value $\lambda$ corresponding to different site occupancy is

$$\lambda = \frac{\Delta G_{ads} - \Delta G_{ads,\max}}{RT} \tag{33}$$

the distribution function of the sites with different adsorption strength [9] takes a form [40]

$$\varphi(\lambda) = \frac{\gamma L}{e^{\gamma\psi} - 1} e^{\gamma\lambda}, 0 \leqslant \lambda \leqslant \psi \tag{34}$$

where $L$ is the total number of surface sites and $\gamma$ is a parameter characterizing the isotherm type [9]. The value of $\gamma$ ranges between −1 and 1 with positive values corresponding to the Freundlich isotherm, while the logarithmic (Temkin) isotherm is obtained when $\gamma = 0$.

Integration of (33) results in an expression for the number of sites corresponding to a particular value of $\lambda$

$$N = \frac{\gamma L}{e^{\gamma\psi} - 1}\int_0^{\lambda} e^{\gamma\lambda} dx = L\frac{e^{\gamma\lambda} - 1}{e^{\gamma\psi} - 1} \tag{35}$$

From the site occupancy (i.e. $\theta = N/L$) an expression for $\lambda$ is [40]

$$\lambda = \frac{1}{\gamma}\ln[\theta(e^{\gamma\psi} - 1) + 1] \tag{36}$$

giving a possibility to express the Gibbs energy of adsorption for different site occupancy or coverage in the classical treatment of adsorption on extended surfaces:

$$\Delta G_{ads} = \Delta G_{ads,\max} + \lambda RT = \Delta G_{ads,\max} + \frac{RT}{\gamma}\ln[\theta(e^{\gamma\psi} - 1) + 1] \tag{37}$$

Because $\Delta G_{ads,\max} < 0$, apparently with an increase of site occupancy $\Delta G_{ads}$ is becoming more positive in line with experimentally observed dependence of adsorption heat on coverage also considering that adsorption entropy has a marginal dependence on the site occupancy. The site occupancy in the context of adsorption of a limited number of adsorbed species per cluster should be viewed not as a coverage in the classical sense, but rather an averaged ratio of a number of adsorbed species $n$ per cluster to the maximum possible number of adsorbed species $n_{\max}$. This ratio $f_n$ depends on the geometrical area of adsorbed species $S_{adsorbed\_species}$, the area of the cluster $S_{nanocluster}$ and the shielding parameter$\phi$:

$$f_n = \frac{n}{n_{\max}} = \frac{n}{\frac{S_{nanocluster}\phi}{S_{adsorbed\_species}}} = \frac{S_{adsorbed\_species}}{S_{nanocluster}\phi} n \tag{38}$$

The parameter $\phi$ takes into account that due to steric constrains and a mismatch in the size of molecules and the cluster not all surface sites are occupied, thus diminishing the maximum number of adsorbed species per cluster. Subsequently the Gibbs energy of adsorption is:

$$\Delta G_{ads} = \Delta G_{ads,\max} + \frac{RT}{\gamma}\ln[n\frac{S_{adsorbed\_species}}{S_{nanocluster}\phi}(e^{\gamma\psi} - 1) + 1] \tag{39}$$

When$\gamma = 0$, eq. (39) cannot be used directly taking instead the form

$$\Delta G_{ads} = \Delta G_{ads,\max} + \lambda RT = \Delta G_{ads,\max} + \psi RT\frac{S_{adsorbed\_species}}{S_{nanocluster}\phi} n \tag{40}$$

## 4. Rate expressions for evenly nonuniform surfaces

For the sake of clarity, only the case for a linear decrease in the Gibbs adsorption energy with site occupancy will be discussed. Subsequently eq. (40) will be used below to define the dependence of the equilibrium and rate constants on the average number of adsorbed species per cluster. Making use of the relationship between equilibrium constants and the Gibbs energy of adsorption one arrives at an expression for the adsorption constant

$$K_{ads} = e^{-\frac{\Delta G_{ads,\max}}{RT}} e^{-\psi\frac{S_{adsorbed\_species}}{S_{nanocluster}\phi} n} = K_{ads,0} e^{-\chi n} \tag{41}$$

with the parameter $\chi$ dependent on the size of adsorbed species and on the cluster dimension

$$\chi = \psi\frac{S_{adsorbed\_species}}{S_{nanocluster}\phi} \tag{42}$$

The pre-exponential factor in eq. (41) corresponds to the maximum value of the Gibbs adsorption energy, which happens on a bare cluster

$$K_{ads,0} = e^{-\frac{\Delta G_{ads,\max}}{RT}} \tag{43}$$

For the case of intrinsic nonuniformity and repulsive lateral interactions, the strongest adsorption corresponds to bare surfaces, as the parameter $\chi$ is positive. The same parameter can be negative for attractive interactions and subsequently for eq. (41) the pre-exponential factor would be

$$K_{ads,0} = e^{-\frac{\Delta G_{ads,0}}{RT}} \tag{44}$$

accounting for the Gibbs adsorption energy on a bare cluster.

Equation of a similar type as eq. (41) was used in [41] for analysis of the optimum catalyst in the case of structure sensitive heterogeneous reactions, when the optimum in the rate was determined for the parameter $z = lnK_{ads}$.

Linear free energy (or Brønsted-Evans-Polanyi) relationships are

widely used in homogeneously and heterogeneously catalyzed reactions [42] linking the rate constants $k$ with equilibrium constants $K$ in a series of analogous elementary reactions:

$$k = gK^{\alpha},\ 0 < \alpha < 1 \tag{45}$$

Subsequently considering eq. (41) and (45) an expression for the rate constant of adsorption is

$$k_{ads} = gK_{ads,0}^{\alpha} e^{-\alpha\chi n} \tag{46}$$

To comply with eq. (41) the desorption rate is then

$$k_{des} = gK_{ads,0}^{\alpha-1} e^{(1-\alpha)\chi n} \tag{47}$$

The notation in eq. (46) and (47) can be slightly modified to be in line with the notation of mechanism (7) where the first route corresponds to adsorption on a bare cluster with $n$ equal to zero

$$k_{+1}^{I} = gK_{1,0}^{\alpha_1} e^{-\alpha_1\chi} e^{-\alpha_1\chi(n^{(I)}-1)} = \left(k_{+1}^{I}\right)' e^{-\alpha_1\chi(n^{(I)}-1)} \tag{48}$$

In this way the route number $N^{(I)}$ is exceeding the number of adsorbed species already present on the surface $n$ by one. In eq. (48) $n^{(I)}$ corresponds to the route $N^{(I)}$ being thus equal to unity (i.e.$n^{(I)} = 1$). Similarly the rate constant for the backward reaction is

$$k_{-1}^{I} = \left(k_{-1}^{I}\right)' e^{(1-\alpha_1)\chi(n^{(I)}-1)} \tag{49}$$

Analogously it holds for the second step:

$$k_{+2}^{I} = \left(k_{+2}^{I}\right)' e^{(1-\alpha_2)\chi(n^{(I)}-1)};\ k_{-2}^{I} = \left(k_{-2}^{I}\right)' e^{-\alpha_2\chi(n^{(I)}-1)} \tag{50}$$

if the values of Polanyi parameter are different for the first and the second step. Otherwise, the expressions for rate constants for different routes can be essentially simplified:

$$\begin{aligned} &k_{+1}^{I} = \left(k_{+1}^{I}\right)' e^{-\alpha\chi(n^{(I)}-1)};\ k_{+1}^{II} = \left(k_{+1}^{I}\right)' e^{-\alpha\chi(n^{(II)}-1)};\\ &k_{+1}^{III} = \left(k_{+1}^{I}\right)' e^{-\alpha\chi(n^{(III)}-1)};\ k_{+1}^{IV} = \left(k_{+1}^{I}\right)' e^{-\alpha\chi(n^{(IV)}-1)}; \end{aligned} \tag{51}$$

with $n^{(I)} = 1, n^{(II)} = 2, n^{(III)} = 3, n^{(IV)} = 4$. Expressions for parameters $U_1$, $U_2$, $U_3$, $U_4$, etc. can be easily obtained considering that the Polanyi parameters are the same for all steps and do not depend on the site occupancy

$$U_1 = \frac{\omega_{+1}^{I} + \omega_{-2}^{I}}{\omega_{+2}^{I} + \omega_{-1}^{I}} = \frac{\left[\left(\omega_{+1}^{I}\right)' + \left(\omega_{-2}^{I}\right)\right] e^{-\alpha\chi(n^{(I)}-1)}}{\left[\left(\omega_{+2}^{I}\right)' + \left(\omega_{.1}^{I}\right)'\right] e^{(1-\alpha)\chi(n^{(I)}-1)}} = \frac{\left[\left(\omega_{+1}^{I}\right)' + \left(\omega_{-2}^{I}\right)\right]}{\left[\left(\omega_{+2}^{I}\right)' + \left(\omega_{.1}^{I}\right)'\right]} e^{-\chi(n^{(I)}-1)} \tag{52}$$

$$U_2 = \frac{\left[\left(\omega_{+1}^{I}\right)' + \left(\omega_{-2}^{I}\right)\right]}{\left[\left(\omega_{+2}^{I}\right)' + \left(\omega_{.1}^{I}\right)'\right]} e^{-\chi(n^{(II)}-1)} = U_1 e^{-\chi(n^{(II)}-1)};\ U_3 = U_1 e^{-\chi(n^{(III)}-1)};\ U_4 = U_1 e^{-\chi(n^{(IV)}-1)} \tag{53}$$

Finally, eq. (20) reflecting the rate in the forward direction when maximum four adsorbed species can be present on a cluster, takes a form

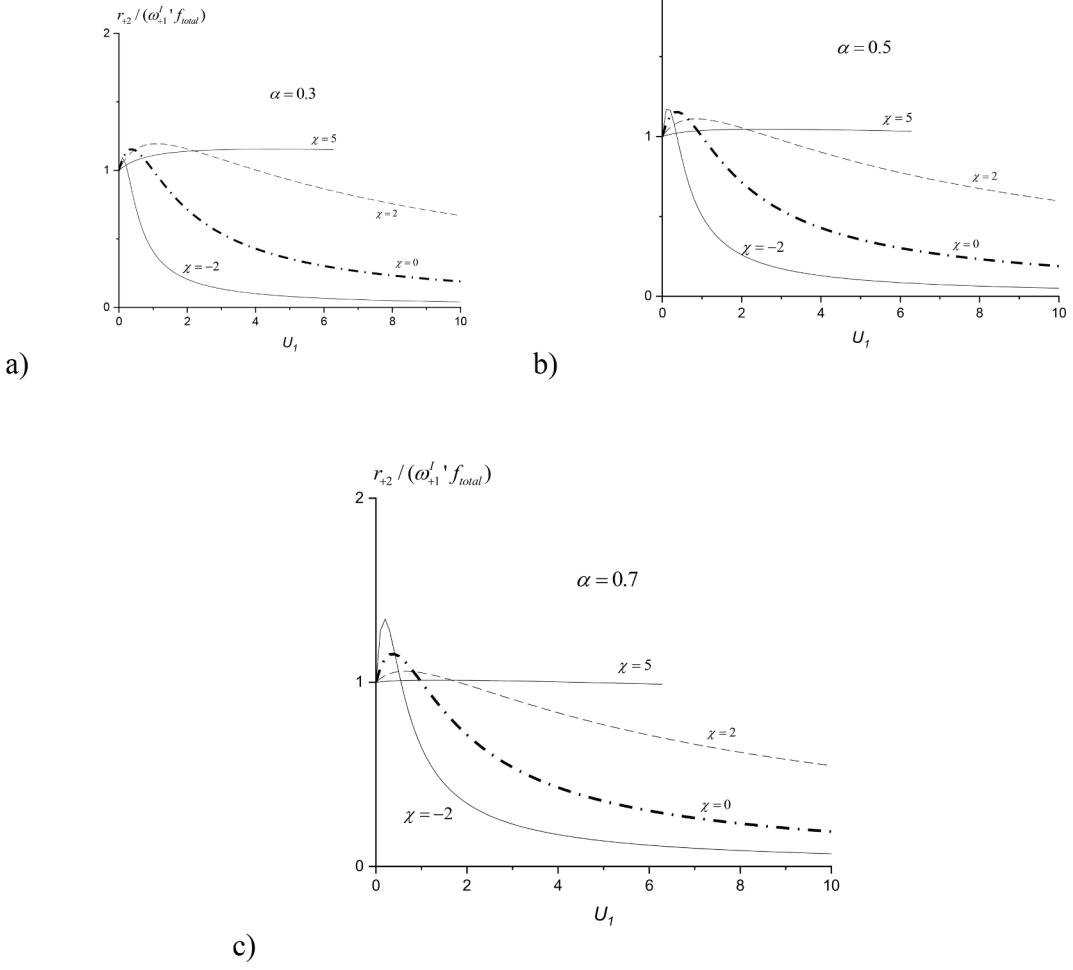


**Fig. 2.** The reaction rates for a cluster with n = 2 as a function of parameter $U_1$ and different values of Polanyi parameter: a) 0.3, b) 0.5, c) 0.7.

$$r_+ = \frac{(\omega^I_{+1})'(1 + U_1 e^{-\alpha\chi} + (U_1)^2 e^{-(2\alpha+1)\chi} + (U_1)^3 e^{-(3\alpha+3)\chi})f_{total}}{1 + U_1 + (U_1)^2 e^{-\chi} + (U_1)^3 e^{-3\chi} + (U_1)^4 e^{-6\chi}} \quad (54)$$

Or in a general case on $n$ species

$$r_+ = \frac{(\omega^I_{+1})'(1 + U_1 e^{-\alpha\chi} + (U_1)^2 e^{-(2\alpha+1)\chi} + \ldots + (U_1)^{n-1} e^{-\chi[\alpha(n-1)+\sum_1^{n-1}(n-1)]})f_{total}}{1 + U_1 + (U_1)^2 e^{-\chi} + \ldots + (U_1)^n e^{-\chi\sum_1^n(n-1)}} \quad (55)$$

In a similar fashion, the rate in the reverse direction in a general form is

$$r_- = \frac{(\omega^I_{-1}U_1 + \omega^{II}_{-2}U_1U_2 + \omega^{III}_{-1}U_1U_2U_3 + .. + \omega^n_{-1}U_1U_2..U_n)f_{total}}{1 + U_1 + U_1U_2 + U_1U_2U_3 + \ldots + U_1U_2U_3\ldots U_n} = \\ = \frac{(\omega^I_{-1})'(U_1 + \ldots + (U_1)^n e^{\chi(1-\alpha)(n-1)-\chi\sum_1^n(n-1)]})f_{total}}{1 + U_1 + (U_1)^2 e^{-\chi} + \ldots + (U_1)^n e^{-\chi\sum_1^n(n-1)}} \quad (56)$$

Manipulation of eqns. (55) and (56) is even more complicated than with eqs. (26) and (27). However, as both equations are a result of the rigorous derivation of the steady-state kinetic expression the Horiuti expression (eq. 25) should be also valid here.

## 5. Dependence on site occupancy: Two species per cluster

For two adsorbed species eq. (55) can be simplified leading to

$$r_+ = \frac{(\omega^I_{+1})'(1 + U_1 e^{-\alpha\chi})f_{total}}{1 + U_1 + (U_1)^2 e^{-\chi}} \quad (57)$$

Numerical analysis of equation (57) will be done below by considering dependencies of the reaction rates as a function of $U_1$ at different values of the Polanyi parameter and $\chi$. When the size of a cluster is increasing, meaning that in general more species can adsorb on the surface, the value of the parameter $\chi$ remains the same as this parameter according to eq. (42) reflects the slope of the Gibbs energy changes with an increase of site occupancy and is proportional to the ratio of a maximal possible difference between Gibbs adsorption energy to the maximal number of adsorbed species.

Fig. 2 illustrates a dependence of the rate (or more precisely the ratio $r_{+2}/(\omega^I_{+1}f_{total})$) as a function of the parameter $U_1$ at different values of the Polanyi parameter. As can be seen from Fig. 2 almost the same behavior is observed at different values of$\alpha$, even if some differences in numerical values could be seen. The reason for such behavior is a small interval of $\alpha$, which was varied within a physically reasonable interval (0.3 to 0.7), and the structure of eq. (57), where for the parameter $\alpha$ to have an impact on the rate, the term $U_1 e^{-\alpha\chi}$ should be significant compared to unity.

When the sites are the same or there are no lateral interactions (e.g. $\chi = 0$) the reaction rate passes through a maximum as a function of $U_1$. Recall that $U_1$ is the ratio of formation to consumption frequencies of steps and in the simplest case of both irreversible steps in a two- step sequence is equal to the ratio of the frequencies for the first and the second step (i.e. $U_1 = \omega^I_{+1}/\omega^I_{+2}$). For a mechanism reflecting isomerization (or cracking) when there is no reactant taking part in the second step (i.e. I* →* +D) or the pressure/concentration of that reactant is constant, the reaction rate in the forward direction passes through a maximum even without any competition of both reactants. Such maxima in the rates, typically attributed to the Langmuir-Hinshelwood type of mechanism, were discussed in the context of cooperative kinetics [24]. It follows from Fig. 2 that strong nonuniformity or lateral interactions (higher values of $\chi$) make the rate maxima less prominent and almost smoothening any dependence at $\chi = 5$.

Besides the reaction order another important global reaction parameter often applied to study reaction mechanisms is the apparent activation energy $E_{a,app}$ defined as

$$E_{a,app} = RT^2(\partial \ln r/\partial T) \quad (58)$$

where R is the gas constant. A rigorous analysis of the apparent activation energy for the two-step sequence performed in [2] gave for a reaction with both irreversible steps

$$E_{a,app} = E_{a,1} + E_{a,2} - \frac{k_1 C_A}{k_1 C_A + k_2 C_B}E_{a,1} - \frac{k_2 C_B}{k_1 C_A + k_2 C_B}E_{a,2} \quad (59)$$

where $E_{a,1}$ and $E_{a,2}$ are the apparent activation energy values for the first and the second step respectively. The cluster size dependence of the activation energy was discussed previously in [43] where it was concluded that the activation energy can either increase or decrease as a function of the cluster size depending on which types of sites (i.e. edges or terraces) the Gibbs energy of adsorption is larger.

The general equation for the two step sequence in the forward direction (eq. 57) can be simplified for the case of both irreversible steps and expressed through the frequencies of steps along the route $N^{(I)}$:

$$r_+ = \frac{(\omega^I_{+1}\omega^I_{+2} + (\omega^I_{+1})^2 e^{-\alpha\chi})f_{total}}{\omega^I_{+1} + \omega^I_{+2} + \frac{(\omega^I_{+1})^2}{\omega^I_{+2}}e^{-\chi}} = \frac{(k_{+1}C_A k_{+2}C_B + (k_{+1}C_A)^2 e^{-\alpha\chi})f_{total}}{k_{+1}C_A + k_{+2}C_B + \frac{(k_{+1}C_A)^2}{k_{+2}C_B}e^{-\chi}} \quad (60)$$

The apparent activation energy is calculated as

$$E_{act,apparent} = RT^2\frac{\partial \ln \frac{(k_{+1}C_A k_{+2}C_B + (k_{+1}C_A)^2 e^{-\alpha\chi})f_{total}}{k_{+1}C_A + k_{+2}C_B + \frac{(k_{+1}C_A)^2}{k_{+2}C_B}e^{-\chi}}}{\partial T} = \quad (61)$$

$$= RT^2\frac{\partial}{\partial T}(\ln(k_{+1}C_A k_{+2}C_B + (k_{+1}C_A)^2 e^{-\alpha\chi}) + \ln f_{total} - \ln(k_{+1}C_A + k_{+2}C_B + \frac{(k_{+1}C_A)^2}{k_{+2}C_B}e^{-\chi}))$$

For a function $U$ it holds that

$$\frac{\partial \ln U}{\partial T} = \frac{\partial \ln U}{\partial U}\frac{\partial U}{\partial T} = \frac{1}{U}\frac{\partial U}{\partial T} \quad (62)$$

Subsequently neglecting dependence of the pre-exponential factor on temperature in $\ln k_{+1}$ in comparison with the exponential term of the Arrhenius equation and considering that the interval between the maximum and minimum values of the Gibbs adsorption energy does not depend on reaction temperature, one gets for different terms in eq. (61):

Combining eq. (61), (63) and (64) the expression for the apparent

$$\frac{\partial}{\partial T}\left(\ln\left(k_{+1}C_Ak_{+2}C_B+\left(k_{+1}C_A\right)^2e^{-\alpha\chi}\right)\right)=\frac{\partial\ln\left(k_{+1}C_Ak_{+2}C_B+\left(k_{+1}C_A\right)^2e^{-\alpha\chi}\right)}{\partial\left(k_{+1}C_Ak_{+2}C_B+\left(k_{+1}C_A\right)^2e^{-\alpha\chi}\right)}\frac{\partial\left(k_{+1}C_Ak_{+2}C_B+\left(k_{+1}C_A\right)^2e^{-\alpha\chi}\right)}{\partial T}=$$
$$=\frac{1}{k_{+1}C_Ak_{+2}C_B+\left(k_{+1}C_A\right)^2e^{-\alpha\chi}}\frac{\partial\left(k_{+1}C_Ak_{+2}C_B+\left(k_{+1}C_A\right)^2e^{-\alpha\chi}\right)}{\partial T}= \tag{63}$$
$$=\frac{C_{A_1}k_{+1}^0k_{+2}^0C_AC_Be^{-\left(E_{+1}+E_{+2}\right)/RT}\frac{E_{+1}+E_{+2}}{RT^2}+\left(k_{+1}^0C_A\right)^2e^{-\alpha\chi}e^{-2E_{+1}/RT}\frac{2E_{+1}}{RT^2}}{k_{+1}C_Ak_{+2}C_B+\left(k_{+1}C_A\right)^2e^{-\alpha\chi}}$$

$$\frac{\partial}{\partial T}\left(\ln\left(k_{+1}C_A+k_{+2}C_B+\frac{\left(k_{+1}C_A\right)^2}{k_{+2}C_B}e^{-\chi}\right)\right)=$$
$$\frac{\partial\ln\left(k_{+1}C_A+k_{+2}C_B+\frac{\left(k_{+1}C_A\right)^2}{k_{+2}C_B}e^{-\chi}\right)}{\partial\left(k_{+1}C_A+k_{+2}C_B+\frac{\left(k_{+1}C_A\right)^2}{k_{+2}C_B}e^{-\chi}\right)}\frac{\partial\left(k_{+1}C_A+k_{+2}C_B+\frac{\left(k_{+1}C_A\right)^2}{k_{+2}C_B}e^{-\chi}\right)}{\partial T}=$$
$$=\frac{1}{k_{+1}C_A+k_{+2}C_B+\frac{\left(k_{+1}C_A\right)^2}{k_{+2}C_B}e^{-\chi}}\frac{\partial\left(k_{+1}C_A+k_{+2}C_B+\frac{\left(k_{+1}C_A\right)^2}{k_{+2}C_B}e^{-\chi}\right)}{\partial T}= \tag{64}$$
$$=\frac{C_Ak_{+1}^0e^{-\mathbf{ERROR!!}E_{+1}/RT}\frac{E_{+1}}{RT^2}+C_Bk_{+2}^0e^{-E_{+2}/RT}\frac{E_{+2}}{RT^2}+\frac{\left(k_{+1}^0C_A\right)^2}{k_{+2}^0C_B}e^{-\chi}e^{\left(-2E_{+1}+E_{+2}\right)/RT}\frac{2E_{+1}-E_{+2}}{RT^2}}{k_{+1}C_A+k_{+2}C_B+\frac{\left(k_{+1}C_A\right)^2}{k_{+2}C_B}e^{-\chi}}$$

activation energy is

$$E_{a,app}=\frac{\left(E_{+1}+E_{+2}\right)k_{+1}C_Ak_{+2}C_B+2E_{+1}\left(k_{+1}C_A\right)^2e^{-\alpha\chi}}{k_{+1}C_Ak_{+2}C_B+\left(k_{+1}C_A\right)^2e^{-\alpha\chi}}-$$
$$-\frac{E_{+1}k_{+1}C_A+E_{+2}k_{+2}C_B+\frac{\left(k_{+1}C_A\right)^2}{k_{+2}C_B}e^{-\chi}\left(2E_{+1}-E_{+2}\right)}{k_{+1}C_A+k_{+2}C_B+\frac{\left(k_{+1}C_A\right)^2}{k_{+2}C_B}e^{-\chi}} \tag{65}$$

which takes the following form

$$E_{a,app}=\frac{\left(E_{+1}+E_{+2}\right)\omega_{+1}\omega_{+2}+2E_{+1}\left(\omega_{+1}\right)^2}{\omega_{+1}\omega_{+2}+\left(\omega_{+1}\right)^2}-$$
$$-\frac{E_{+1}\omega_{+1}\omega_{+2}+E_{+2}\left(\omega_{+2}\right)^2+\left(\omega_{+1}\right)^2\left(2E_{+1}-E_{+2}\right)}{\omega_{+1}\omega_{+2}+\left(\omega_{+2}\right)^2+\left(\omega_{+1}\right)^2} \tag{66}$$

when the surface of a cluster can accommodate two adsorbed species, which react independent on the presence of each other (i.e.$\chi=0$). Alternatively a very high value of $\chi=0$ implies that the second adsorbed specie is not reactive $e^{-\alpha\chi}\approx0$ and eq. (65) can be reduced to the classical expression for the two-step sequence [2]:

$$E_{a,app}=E_{+1}+E_{+2}-\frac{E_{+1}\omega_{+1}+E_{+2}\omega_{+1}}{\omega_{+1}+\omega_{+2}}=\frac{\omega_{+2}}{\omega_{+1}+\omega_{+2}}E_{+1}+\frac{\omega_{+1}}{\omega_{+1}+\omega_{+2}}E_{+2} \tag{67}$$

## 6. Dependence on site occupancy: Beyond two species per cluster

To align the theoretical discussion on the dependence of the rate on the site occupancy with some practical cases, adsorption of isoeugenol on a surface of a metal catalyst will be considered. Hydrodeoxygenation (HDO) of this compound originating from lignin has been extensively studied in the literature [44,45]. While virtually placing several molecules of isoeugenol on a flat surface, it can be easily obtained that the geometrical surface area of 6 adsorbed species (Fig. 3) is ca. 4 nm$^2$, which for a half-spherical particle and the shielding parameter $\phi$ equal to 0.7, typical for aromatic compounds [40], corresponds to a cluster diameter of ca. 2 nm. Catalysts with such and even lower dimensions of

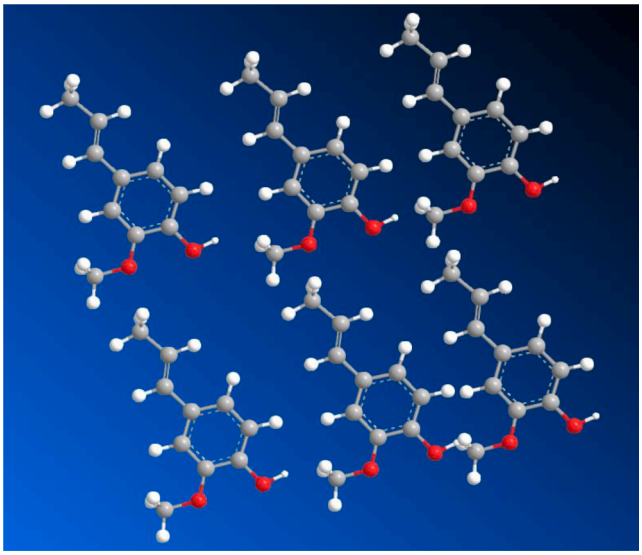

**Fig. 3.** Atop view of 6 isoeugenol molecules.

**Table 1**
Kinetic expressions for different maximal adsorbed species.

| n | Expression for the forward reaction rate |
|---|---|
| 1 | $r_+ = \frac{(\omega^I_{+1})' f_{total}}{1+U_1}$ |
| 2 | $r_+ = \frac{(\omega^I_{+1})'(1+U_1 e^{-\alpha\chi}) f_{total}}{1+U_1+(U_1)^2 e^{-\chi}}$ |
| 3 | $r_+ = \frac{(\omega^I_{+1})'(1+U_1 e^{-\alpha\chi}+(U_1)^2 e^{-(2\alpha+1)\chi}) f_{total}}{1+U_1+(U_1)^2 e^{-\chi}+(U_1)^3 e^{-3\chi}}$ |
| 4 | $r_+ = \frac{(\omega^I_{+1})'(1+U_1 e^{-\alpha\chi}+(U_1)^2 e^{-(2\alpha+1)\chi}+(U_1)^3 e^{-(3\alpha+3)\chi}) f_{total}}{1+U_1+(U_1)^2 e^{-\chi}+(U_1)^3 e^{-3\chi}+(U_1)^4 e^{-6\chi}}$ |
| 5 | $r_+ = \frac{(\omega^I_{+1})'(1+U_1 e^{-\alpha\chi}+(U_1)^2 e^{-(2\alpha+1)\chi}+(U_1)^3 e^{-(3\alpha+3)\chi}+(U_1)^4 e^{-\chi[4\alpha+6]}) f_{total}}{1+U_1+(U_1)^2 e^{-\chi}+(U_1)^3 e^{-3\chi}+(U_1)^4 e^{-6\chi}+(U_1)^5 e^{-10\chi}}$ |
| 6 | $r_+ = \frac{(\omega^I_{+1})'(1+U_1 e^{-\alpha\chi}+(U_1)^2 e^{-(2\alpha+1)\chi}+(U_1)^3 e^{-(3\alpha+3)\chi}+(U_1)^4 e^{-\chi[4\alpha+6]}+(U_1)^5 e^{-\chi[5\alpha+10]}) f_{total}}{1+U_1+(U_1)^2 e^{-\chi}+(U_1)^3 e^{-3\chi}+(U_1)^4 e^{-6\chi}+(U_1)^5 e^{-10\chi}+(U_1)^6 e^{-15\chi}}$ |

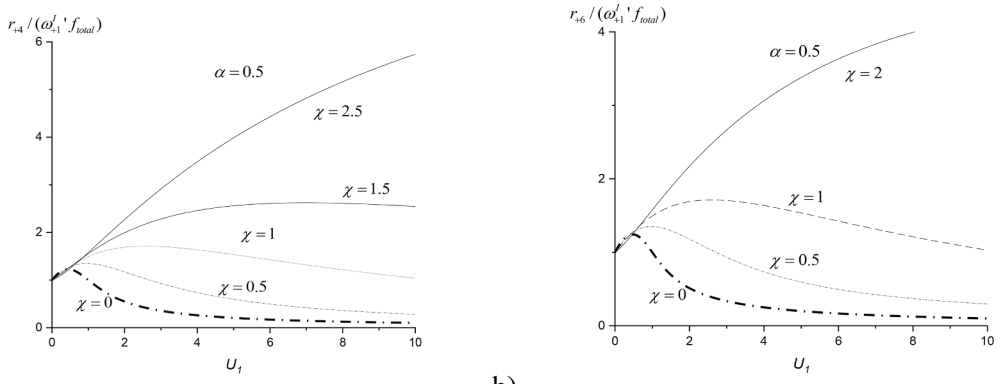


a) b)

**Fig. 4.** The reaction rates for a cluster with a) n = 4 and b) n = 6 as a function of the parameter $U_1$ and the Polanyi parameter equal to 0.5.

**Table 2**
Kinetic expressions for the relative ratios of rates.

| n | Expression for the relative forward reaction rates |
|---|---|
| 1 | $r_{+(1/1)} = 1$ |
| 2 | $r_{+(2/1)} = \frac{1+U_1(1+e^{-\alpha\chi})+(U_1)^2 e^{-\alpha\chi}}{1+U_1+(U_1)^2 e^{-\chi}}$ |
| 3 | $r_{+(3/1)} = \frac{1+U_1(1+e^{-\alpha\chi})+(U_1)^2(e^{-(2\alpha+1)\chi}+e^{-\alpha\chi})+(U_1)^3 e^{-(2\alpha+1)\chi}}{1+U_1+(U_1)^2 e^{-\chi}+(U_1)^3 e^{-3\chi}}$ |
| 4 | $r_{+(4/1)} = \frac{1+U_1(1+e^{-\alpha\chi})+(U_1)^2(e^{-\alpha\chi}+e^{-(2\alpha+1)\chi})+(U_1)^3(e^{-(2\alpha+1)\chi}+e^{-(3\alpha+3)\chi})+(U_1)^4 e^{-(3\alpha+3)\chi}}{1+U_1+(U_1)^2 e^{-\chi}+(U_1)^3 e^{-3\chi}+(U_1)^4 e^{-6\chi}}$ |
| 5 | $r_{+(5/1)} = \frac{1+U_1(1+e^{-\alpha\chi})+(U_1)^2(e^{-\alpha\chi}+e^{-(2\alpha+1)\chi})+(U_1)^3(e^{-(2\alpha+1)\chi}+e^{-(3\alpha+3)\chi})+(U_1)^4(e^{-\chi[4\alpha+6]}+e^{-(3\alpha+3)\chi})+(U_1)^5 e^{-\chi[4\alpha+6]}}{1+U_1+(U_1)^2 e^{-\chi}+(U_1)^3 e^{-3\chi}+(U_1)^4 e^{-6\chi}+(U_1)^5 e^{-10\chi}}$ |
| 6 | $r_{+(6/1)} = \frac{1+U_1(1+e^{-\alpha\chi})+(U_1)^2(e^{-\alpha\chi}+e^{-(2\alpha+1)\chi})+(U_1)^3(e^{-(2\alpha+1)\chi}+e^{-(3\alpha+3)\chi})+(U_1)^4(e^{-\chi[4\alpha+6]}+e^{-(3\alpha+3)\chi})+(U_1)^5(e^{-\chi[4\alpha+6]}+e^{-\chi[5\alpha+10]})+(U_1)^6 e^{-\chi[5\alpha+10]}}{1+U_1+(U_1)^2 e^{-\chi}+(U_1)^3 e^{-3\chi}+(U_1)^4 e^{-6\chi}+(U_1)^5 e^{-10\chi}}$ |

metal clusters are often utilized in HDO of isoeugenol. It could be thus interesting to analyze dependence of the reaction rate on the size of clusters. Table 1 lists the rate expressions for different maximal values of adsorbed species from 1 to 6 reflecting eventually the corresponding cluster size.

The rates on a cluster with four and six adsorbed species as a function of the parameter $U_1$ are presented in Fig. 4 for the Polanyi parameter equal to 0.5.

According to Fig. 4 at sufficient values of $\chi$ the maxima in the rates can be rather broad expanding over a broad range of the parameter $U_1$. This is an interesting observation illustrating that a very rich kinetic behavior exhibiting maxima in the reaction rates, often associated with the Langmuir-Hinshelwood type of mechanisms, can be expected for the two-step sequence without a direct competition of reacting molecules when the size of clusters is changing. The latter leads to a larger number of adsorbed species which are accommodated on the surface altering the kinetic expression.

A visual comparison between Fig. 4 and Fig. 2b illustrates that the dependence for the cluster with maximum two adsorbed species on the parameter $U_1$ looks less pronounced than for more adsorbed species. This is manifested by much larger changes in the absolute values of the rates at similar values of $\chi$ when more adsorbed species can be accommodated on a cluster.

To quantify these differences, the relative ratios of rates on clusters with cooperative behavior compared to a conventional expression for a two-step sequence are listed in Table 2. Subsequently the equations in Table 2 can be compared for different values of $n$ and thus the cluster size keeping the value of parameter $\chi$ the same.

Such analysis is shown in Fig. 5 for the relative ratio of the rates when two or one adsorbed intermediates can be accommodated on the

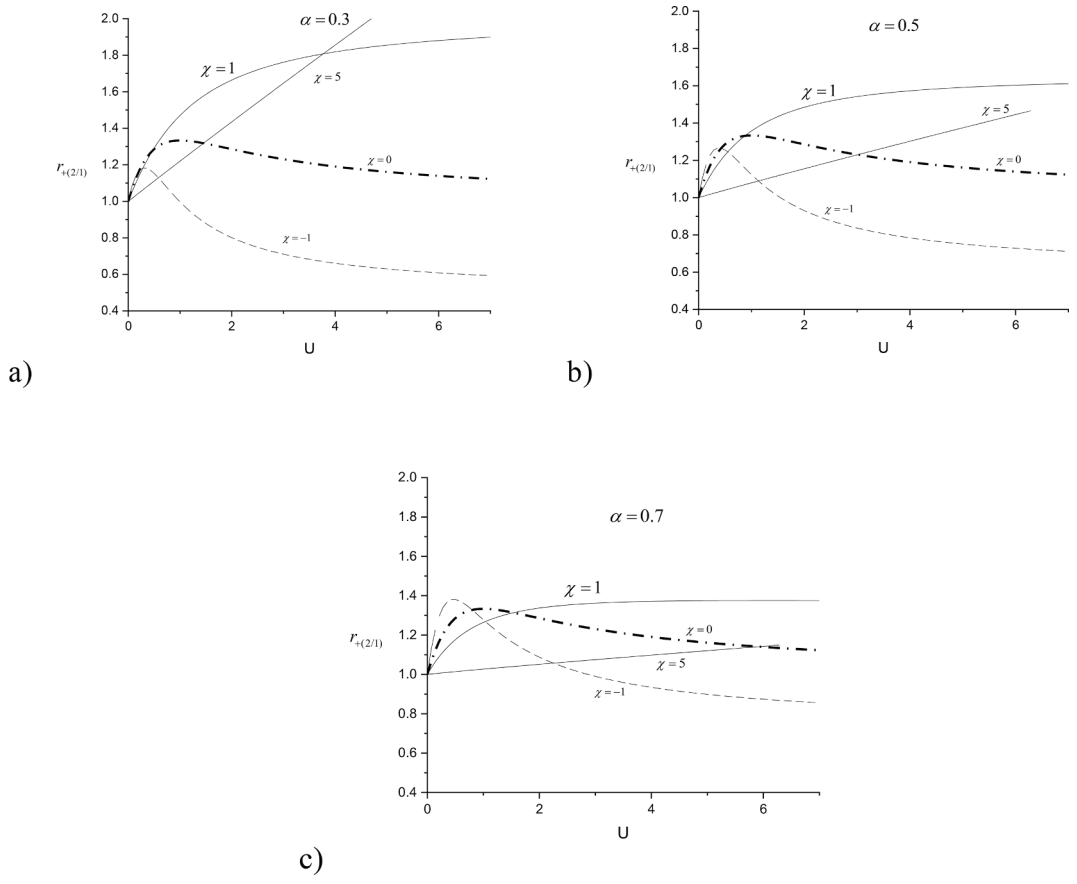


**Fig. 5.** The relative ratio of rates for a cluster with n = 2 as a function of parameter U and different values of Polanyi parameter: a) 0.3, b) 0.5, c) 0.7.

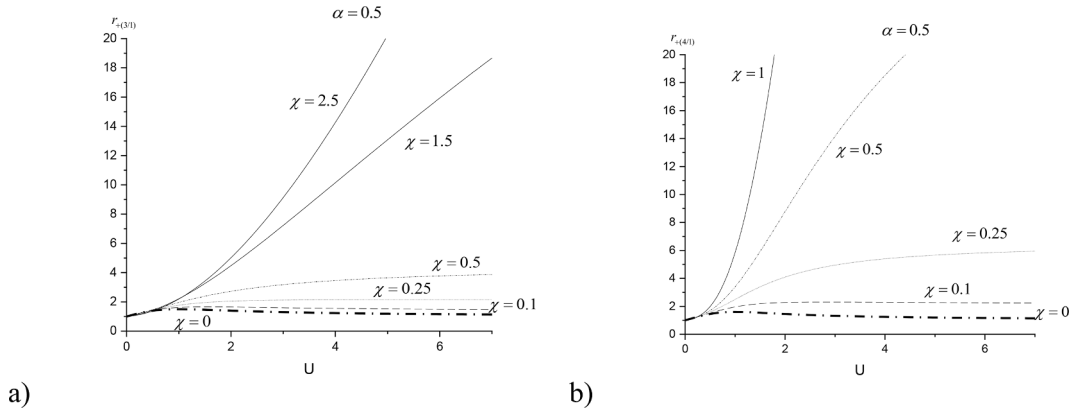


**Fig. 6.** The relative ratio of rates for a cluster with a) n = 3, b) n = 4 as a function of parameter U and different values of nonuniformity parameter$\chi$.

catalyst surface and considering several values of the Polanyi parameter. As quite often the value of this parameter is close to 0.5, Fig. 6 addresses this case for the ratio of the rates when three (or four) intermediates are adsorbed compared with the base case of a single intermediate adsorbed on the surface.

As can be seen from Fig. 5 that for the case of two adsorbed species per cluster and the Polanyi parameter equal to 0.5, i.e. the one experimentally often obtained [9], the changes in the ratio of rates depending on the value of $U$ (and thus on such reaction parameters as reactants concentrations) are rather moderate for the uniform surface without any lateral interactions ($\chi = 0$). Positive values of the nonuniformity parameter $\chi$ imply an increase in the relative rates due to cooperative behavior, while maxima could be observed for uniform surfaces and also for negative values of the nonuniformity parameter$\chi$.

## 7. Illustration of the model applicability: Cluster size dependent reduction of resazurin

The catalytic properties of gold are known to be very sensitive to the size of gold clusters [46–48]. Not only the reaction rates, but kinetic regularities can undergo substantial differences when the size of gold Au15 cluster stabilized with 3-mercaptopropionic acid is increased to Au18 and Au25 [49]. For the former case in reduction of a nonfluorescent resazurin (Fig. 7a) by hydroxylamine Au15 exhibited maxima in the rates as a function of both reactants allowing the authors to conclude a competitive Langmuir-Hinshelwood (LH) type of kinetics. On the

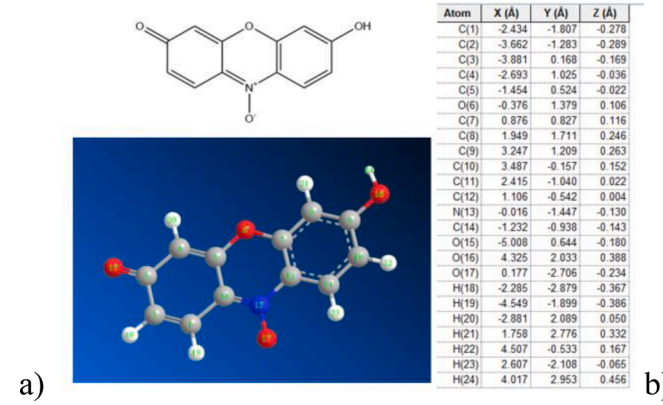


| Atom | X (Å) | Y (Å) | Z (Å) |
|---|---|---|---|
| C(1) | -2.434 | -1.807 | -0.278 |
| C(2) | -3.662 | -1.283 | -0.289 |
| C(3) | -3.881 | 0.168 | -0.169 |
| C(4) | -2.693 | 1.025 | -0.036 |
| C(5) | -1.454 | 0.524 | -0.022 |
| O(6) | -0.376 | 1.379 | 0.106 |
| C(7) | 0.876 | 0.827 | 0.116 |
| C(8) | 1.949 | 1.711 | 0.246 |
| C(9) | 3.247 | 1.209 | 0.263 |
| C(10) | 3.487 | -0.157 | 0.152 |
| C(11) | 2.415 | -1.040 | 0.022 |
| C(12) | 1.106 | -0.542 | 0.004 |
| N(13) | -0.016 | -1.447 | -0.130 |
| C(14) | -1.232 | -0.938 | -0.143 |
| O(15) | -5.008 | 0.644 | -0.180 |
| O(16) | 4.325 | 2.033 | 0.388 |
| O(17) | 0.177 | -2.706 | -0.234 |
| H(18) | -2.285 | -2.879 | -0.367 |
| H(19) | -4.549 | -1.899 | -0.386 |
| H(20) | -2.881 | 2.089 | 0.050 |
| H(21) | 1.758 | 2.776 | 0.332 |
| H(22) | 4.507 | -0.533 | 0.167 |
| H(23) | 2.607 | -2.108 | -0.065 |
| H(24) | 4.017 | 2.953 | 0.456 |

**Fig. 7.** Resazurin: a) the chemical formula with the atom coordinates, b) optimized structures for adsorption of resazurin on gold clusters of different sizes, reproduced with permission from [49].

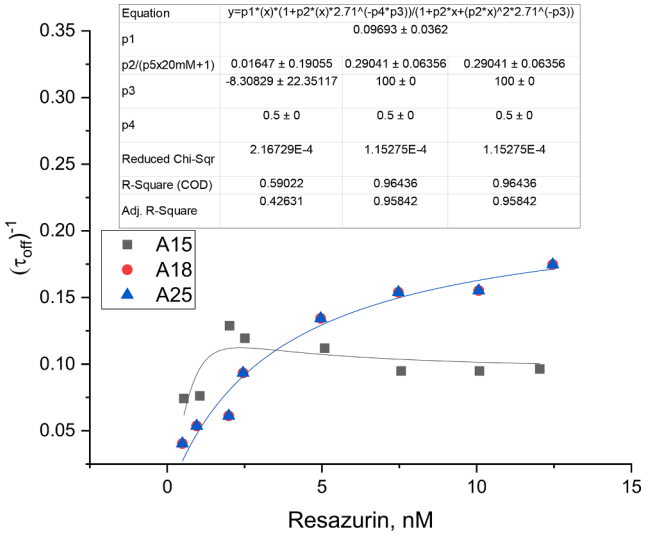


**Fig. 8.** Kinetic data for resazurin reduction with hydroxylamine [49]. Dependence of the product formation rate on resazurin concentration at fixed hydroxylamine concentration of 20 mM.

contrary for Au18 and Au25 clusters the kinetic behavior was different and the reaction rates levelled off at high concentration of reactants formally similar to a noncompetitive LH kinetics.

Quite often differences in the catalytic behavior upon minute variations of the cluster size are attributed exclusively to the properties of gold. Such a switch in the mechanism might sound counterintuitive when the average cluster size increases from 0.78 to just 0.84 nm [49] taking into account a substantial distribution of cluster sizes.

An alternative explanation not involving a complete switch of the reaction mechanism with a minor change in the size can be related to geometrical restrictions, namely a difference in the number of molecules which adsorb on the surface of Au15 and A18 clusters. Let us consider first the DFT calculations for A15 and A25 clusters (Fig. 7) reported in [49].

As can be seen from Fig. 7, a large size of a cluster in fact implies a more flat adsorption and thus just one adsorbed reactant per cluster. On the contrary a more tilted adsorption of resazurin on Au15 allows accommodation of a second reactant molecule, which would lead to the rate expression

$$r_+ = \frac{(k^I_{+1}C_R)(1+\frac{k^I_{+1}C_R}{k^I_{+2}C_{HA}+k^I_{-1}}e^{-\alpha\chi})f_{total}}{1+\frac{k^I_{+1}C_R}{k^I_{+2}C_{HA}+k^I_{-1}}+\left(\frac{k^I_{+1}C_R}{k^I_{+2}C_{HA}+k^I_{-1}}\right)^2 e^{-\chi}} = \frac{(p_1C_R)(1+\frac{p_2C_R}{p_5C_{HA}+1}e^{-p_4p_3})}{1+\frac{p_2C_R}{p_5C_{HA}+1}+\left(\frac{p_2C_R}{p_5C_{HA}+1}\right)^2 e^{-p_3}} \quad (68)$$

Eq. (68) is derived assuming the overall irreversibility of the reaction and neglecting the influence of the product on the rate of the forward reaction. In q. (68) $C_R$ and $C_{HA}$ correspond to the concentration of resazurin and hydroxylamine, respectively, and

$$p_1 = k^I_{+1}f_{total};\quad p_2 = k^I_{+1}/k^I_{-1};\quad p_3 = \chi;\quad p_4 = \alpha;\quad p_5 = k^I_{+2}/k^I_{-1} \quad (69)$$

For the data fitting with Origin 2019 software the Polanyi parameter was fixed to 0.5, while a high value of the parameter $p_3$ in the calculations for Au18 and Au25 (i.e. 100) was needed to essentially reduce eq. (68) to a classical two-step sequence. In the data fitting to avoid a correlation between parameters a lumped parameter $p_2/(p_5C_{HA}+1)$ was calculated as the concentration of the reductant was the same. As can be seen from Fig. 8 an overall good description was obtained for both types of kinetic behavior with the same two-step sequence mechanism but different number of adsorbed species per cluster adhering to the geometric requirements of both the cluster and the substrate. A particular feature of the calculation results for Au15 is that $p_3$ and thus $\chi$ are negative as could be expected from the theoretical simulations in the previous section.

The mechanism of resazurin reduction with hydroxylamine can be more complicated than just a two-step sequence and the analysis above does not necessarily rule out a mechanism based on the competitive Langmuir-Hinshelwood model, but rather illustrates an approach how to treat catalytic kinetics for cases when geometrical restrictions and a limited number of adsorbed species per cluster should be taken into account.

The current example illustrates applicability of the model to the resazurin reduction reaction where a substantially different kinetic behavior was observed for a large organic molecule on clusters of the size similar to the size of the reactant. It can be anticipated that the mathematical treatment developed here can be used for similar cases of heterogeneous catalytic reactions when just few adsorbed species can be accommodated on a nanocluster, as well as in the cases of reactions in confined spaces, e.g. in the pores of zeolites, where confinement of adsorbed species within a pore clearly can influence catalytic behavior [50].

## 8. Conclusions

Kinetics on nanoclusters capable of accommodating, due to the size restrictions, only few adsorbed molecules, is discussed for the two-step mechanism. In such a mechanism one of the reactants first forms an adsorbed intermediate, which is further transformed in a subsequent step by reacting with the second reactant.

The work represent an extension of the previously published theoretical development for a case when a nanocluster can accommodate only two adsorbed reaction intermediates. In the current study a general

analysis is provided for clusters with more adsorbed molecules also considering that the kinetic parameters are dependent on the cluster occupancy.

Derivation of the reaction rate expressions is done for a case with four adsorbed species on a cluster and is generalized for the $n$ species adsorbed on the catalyst surface. In this general case a potentially large number of kinetic parameters, specific for different site occupancy, implies a strong correlation between such parameters.

Therefore, for nanoclusters with a limited number of adsorbed species per cluster, dependence of the reaction parameters on the cluster occupancy was considered by relating the adsorption energy and the average number of adsorbed species per cluster across all clusters.

Subsequently instead of the coverage, routinely used in heterogeneous catalytic kinetics, the site occupancy concept was used reflecting the averaged ratio of a number of adsorbed species $n$ per cluster to the maximum possible number of adsorbed species $n_{max}$. The latter is a function of the geometrical area of adsorbed species, the cluster area and shielding of adsorbed species by those already present on the surface.

Numerical analysis is provided for the dependence of the rate vs site occupancy as a function of ratio between frequencies for the formation to consumption steps for different numbers of species per cluster, ranging from 2 to 6.

For a chemical reaction reflecting isomerization or cracking, the reaction rate in the forward direction passes through a maximum, typically attributed to the Langmuir-Hinshelwood kinetics. Strong nonuniformity or lateral interactions make the rate maxima less prominent at high values of the nonuniformity parameter.

Analysis for the relative ratio of the rates when several or alternatively just one adsorbed intermediate can be accommodated on the catalyst surface illustrates that changes in the ratio of rates depending on the reactants concentrations are rather moderate for the uniform surface without any lateral interactions, being more profound for non-ideal surfaces.

An illustration of dramatic changes in the kinetic regularities upon subtle alterations of the cluster size is provided using reduction of a nonfluorescent resazurin by hydroxylamine on Au as an example. Very large differences in the kinetic behavior for gold clusters of 0.78 and 0.84 nm could be explained by a possibility of two species adsorption on a smaller cluster in a tilted position, compared to a more flat orientation on a marginally larger cluster. A slower rate for the smaller cluster and a maximum as a function of the substrate concentration can originate from geometrical restrictions, i.e. a difference in the number of molecules which can adsorb on these clusters.

Numerical analysis of the experimental data was performed to support the theoretical analysis.

## Declaration of Competing Interest

The authors declare that they have no known competing financial interests or personal relationships that could have appeared to influence the work reported in this paper.

## Data availability

No data was used for the research described in the article.

## References


[1] D.Y. Murzin, T. Salmi, Catalytic Kinetics, Chemistry and Engineering, 2d Edition, Elsevier, 2016.
[2] G. Marin, G.S. Yablonsky, D. Constales, Kinetics of Chemical Reactions, Decoding complexity, 2 ed., Wiley, 2019.
[3] B. Punia, S. Chaudhury, A.B. Kolomeisky, Microscopic Mechanisms of Cooperative Communications with Single Nanocatalysts, PNAS 119 (3) (2022) 1–7.
[4] B. Dong, N. Mansour, Y. Pei, Z. Wang, T. Huang, S.L. Filbrun, M. Chen, X. Cheng, M. Pruski, W.Y. Huang, N. Fang, Single molecule investigation of nanoconfinement hydrophobicity in heterogeneous catalysis, J. Am. Chem. Soc. 142 (2020) 13305–13309.
[5] N.K. Razdan, A. Bhan, Kinetic Descriptions of Site Ensembles on Catalytic Surfaces, PNAS 118 (2021) e2019055118.
[6] N.K. Razdan, A. Bhan, Catalytic Site Ensembles: A Context to Reexamine the Langmuir-Hinshelwood Kinetic Description, J. Catal. 404 (2021) 726–744.
[7] I. Langmuir, The adsorption of gases on plane surfaces of glass, mica and platinum, J. Am. Chem. Soc. 40 (1918) 1361–1403.
[8] J. Horiuti, T. Nakamura, On the theory of heterogeneous catalysis, Adv. Catal. 17 (1967) 1–74.
[9] M.I. Temkin, The kinetics of some industrial heterogeneous catalytic reactions, Adv. Catal. 28 (1979) 173–291.
[10] A.Y. Meyer, Molecular Mechanics and Molecular Shape. III. Surface Area and Cross-Sectional Areas of Organic Molecules, J. Comput. Chem. 7 (1986) 144–152.
[11] N.D. Shcherban, P. Mäki-Arvela, A. Aho, S.A. Sergiienko, M.A. Skoryk, E. Kolobova, I.L. Simakova, K. Eränen, A. Smeds, J. Hemming, D.Y. Murzin, Preparation of Betulone via Betulin Oxidation over Ru Nanoparticles Deposited on Graphitic Carbon Nitride, Catal. Lett. 149 (2019) 723–732.
[12] L. Liu, A. Corma, Isolated Metal Atoms and Clusters for Alkane Activation: Translating Knowledge from Enzymatic and Homogeneous to Heterogeneous Systems, Chem 7 (2021) 2347–2384.
[13] M.K. Samantaray, V. D'Elia, E. Pump, L. Falivene, M. Harb, S.O. Chikh, L. Cavallo, J.M. Basset, The comparison between single atom catalysis and surface organometallic catalysis, Chem. Rev. 120 (2020) 734–813.
[14] S.K. Kaiser, Z. Chen, D. Faust Akl, S. Mitchell, J. Pérez-Ramírez, Single-Atom Catalysts across the Periodic Table, Chem. Rev. 120 (2020) 11703–11809.
[15] H.P. Lu, L. Xun, X.S. Xie, Single-Molecule Enzymatic Dynamics, Science 282 (1998) 1877–1882.
[16] S.C. Kou, B.J. Cherayil, W. Min, B.P. English, X.S. Xie, Single-molecule Michaelis-Menten Equations, J. Phys. Chem. B 109 (2005) 19068–19081.
[17] R. Ye, X. Mao, X. Sun, P. Chen, Analogy between Enzyme and Nanoparticle Catalysis: A Single-Molecule Perspective, ACS Catal. 9 (2019) 1985–1992.
[18] N. Zou, X. Zhou, G. Chen, N.M. Andoy, W. Jung, G. Liu, P. Chen, Cooperative Communication within and between Single Nanocatalysts, Nat. Chem. 10 (2018) 607–614.
[19] S. Chaudhury, D. Singh, A.B. Kolomeisky, Theoretical Investigations of the Dynamics of Chemical Reactions on Nanocatalysts with Multiple Active Sites, J. Phys. Chem. Lett. 11 (2020) 2330–2335.
[20] D.Y. Murzin, On Validity of Langmuir Adsorption on Supported Nanoparticles, React. Kinet. Catal. Lett. 91 (2007) 37–43.
[21] D.Y. Murzin, Kinetics of Catalytic Reactions on Nanoclusters, Langmuir 26 (2010) 4854–4859.
[22] M.I. Temkin, Optimal Catalyst of a Two-Step Reaction, Kinet. Katal. 25 (1984) 299–305.
[23] M. Boudart, K. Tamaru, The Step that Determines the Rate of a Single Catalytic Cycle, Catal. Lett. 9 (1991) 15–22.
[24] Murzin, D.Yu., Cooperative Catalytic Nanokinetics, Chemical Engineering Science, 2022, 256, 117684 (1-15).
[25] J. Horiuti, S. Enomoto, Stoichiometric Number and Universal Kinetic Law in the Neighbourhood of Equilibrium. II, Proc. Japan Acad. 29 (1953) 164–168.
[26] M.I. Temkin, Kinetics of Stationary Reactions, Dokl. Akad. Nauk USSR 152 (1963) 156–159.
[27] D.Y. Murzin, Kinetic analysis of cluster size dependent activity and selectivity, J. Catal. 276 (2010) 85–91.
[28] D.Y. Murzin, On Cluster Size Dependent Activity and Selectivity in Heterogeneous Catalysts, Catal. Lett. 142 (2012) 1279–1285.
[29] D.Y. Murzin, Cluster size Dependent Kinetics: Analysis of Different Reaction Mechanisms, Cat. Lett 145 (2015) 1948–1954.
[30] Murzin, D. Yu. Kinetics of Cluster Shape Sensitive Heterogeneous Catalytic Reactions, Chem. Eng. J., 2021, 425, 130642 (1-13).
[31] P.V. Markov, I.S. Mashkovsky, G.O. Bragina, J. Wärnå, E.V. Gerasimov, V. I. Bukhtiyarov, A.Y. Stakheev, D.Y. Murzin, Particle Size Effect in Liquid-Phase Hydrogenation of Phenylacetylene over Pd Catalysts: Experimental Data and Theoretical Analysis, Chem. Eng. J. 358 (2019) 520–530.
[32] Markov, P. V.; Mashkovsky, I. S.; Bragina, G.O.; Wärnå, J.; Bukhtiyarov, V. I.; Stakheev, A.Yu.; Murzin, D. Yu. Experimental and Theoretical Analysis of Particle Size Effect in Liquid-Phase Hydrogenation of Diphenylacetylene, Chem. Eng. J., 2021, 404, 126409 (1-11).
[33] A.V. Rassolov, I.S. Mashkovsky, G.O. Bragina, G.N. Baeva, P.V. Markov, N. S. Smirnova, J. Wärnå, A.Y. Stakheev, D.Y. Murzin, Kinetics of liquid-phase diphenylacetylene hydrogenation on "single-atom alloy" Pd-Ag catalyst: experimental study and kinetic analysis, Mol. Catal. 506 (2021), 111550.
[34] A.V. Rassolov, I.S. Mashkovsky, G.N. Baeva, G.O. Bragina, N.S. Smirnova, P. V. Markov, J. Wärnå, A.V. Bukhtiyarov, A.Y. Stakheev, D.Y. Murzin, Liquid-phase Hydrogenation of 1-Phenyl-1-Propyne on the $Pd_1Ag_3/Al_2O_3$ single-Atom Alloy Catalyst: Kinetic Modeling and the Reaction Mechanism, Nanomater. 11 (2021) 3286.
[35] D.Y. Murzin, Thermodynamic Analysis of Nanoparticle Size Effect on Catalytic Kinetics, Chem. Eng. Sci. 64 (2009) 1046–1052.
[36] D.Y. Murzin, V.N. Parmon, Quantification of Cluster Size Effect (Structure Sensitivity) in Heterogeneous Catalysis, Catal.-Spec. Period. Rep., RSC 23 (2011) 179–203.
[37] Zeldovich, Ya.B. On the Theory of the Freundlich Adsorption Isotherm. Selected Works of Yakov Borisovich Zeldovich, Volume I: Chemical Physics and Hydrodynanics, edited by R.A. Sunyaev, Princeton: Princeton University Press, 2014, pp. 58-67. doi:10.1515/9781400862979.58.

[38] D.Y. Murzin, Modeling of Adsorption and Kinetics in Catalysis over Induced Nonuniform Surfaces: Surface Electronic Gas Model, Ind. Eng. Chem. Res. 34 (1995) 1208–1218.
[39] S.J. Lombardo, A.-T. Bell, A Review on Theoretical Models of Adsorption, Diffusion, Desorption, and Reaction of Gases on Metal Surfaces, Sur. Sci. Rep. 13 (1991) 1–72.
[40] Y.S. Snagovskii, G.M. Ostrovskii, Modelling of Kinetics of Heterogeneous Catalytic Processes, Chimia, Moscow (1976) 248 pp.
[41] D.Y. Murzin, On the Optimum Catalyst for Structure Sensitive Heterogeneous Catalytic Reactions, React. Kinet. Mech. Catal. 131 (2020) 5–17.
[42] K.J. Laidler, Chemical Kinetics, Harper-Collins, 1987.
[43] D.Y. Murzin, On apparent activation energy of structure sensitive heterogeneous catalytic reactions, Cat. Lett. 149 (2019) 1455–1463.
[44] M. Alda-Onggar, P. Mäki-Arvela, K. Eränen, A. Aho, J. Hemming, P. Paturi, M. Peurla, M. Lindblad, I.L. Simakova, D.Y. Murzin, Hydrodeoxygenation of Isoeugenol over Alumina Supported Ir-, Pt- and Re Catalysts, ACS Sust. Chem. Eng. 6 (2018) 16205–16218.
[45] M.E. Martinez-Klimov, M. Mäki-Arvela, Z. Vajglová, M. Alda-Onggar, I. Angervo, N. Kumar, K. Eränen, M. Peurla, M. Calimli, J. Muller, A. Shchukarev, I. L. Simakova, D.Yu Murzin, Hydrodeoxygenation of Isoeugenol over Carbon-Supported Pt and Pt-Re Catalysts for Production of Renewable Jet Fuel, Energy Fuels 35 (2021) 17755–17768.
[46] G.J. Hutchings, Vapor Phase Hydrochlorination of Acetylene: Correlation of Catalytic Activity of Supported Metal Chloride Catalysts, J. Catal. 96 (1985) 292–295.
[47] M. Haruta, N. Yamada, T. Kobayashi, S. Iijima, The Activity of the Tetrahedral Au20 Cluster: Charging and Impurity Effects, J. Catal. 115 (1989) 301–309.
[48] M.C. Haruta, Chance and necessity: my encounter with gold catalysts, Angew. Chem., Int. Ed. 53 (2014) 52–56.
[49] Y. Zhang, P. Song, T. Chen, X. Liu, T. Chen, Z. Wu, Y. Wang, J. Xie, W. Xu, Unique Size-dependent Nanocatalysis Revealed at the Single Atomically Precise Gold Cluster Level, PNAS 115 (2019) 10588–10593.
[50] R. Gounder, E. Iglesia, Catalytic Consequences of Spatial Constraints and Acid Site Location for Monomolecular Alkane Activation on Zeolites, J. Am. Chem. Soc. 131 (2009) 1958–1971.